Carbohydrate Polymers 92 (2013) 2299–2305

Contents lists available at SciVerse ScienceDirect

Carbohydrate Polymers

journal homepage: www.elsevier.com/locate/carbpol

Potential of using multiscale kenaf fibers as reinforcing filler in cassava starch-kenaf biocomposites

Siti Yasmine Zanariah Zainuddin [a], Ishak Ahmad [a,*], Hanieh Kargarzadeh [a], Ibrahim Abdullah [a], Alain Dufresne [b]

[a] School of Chemical Science and Food Technology, Universiti Kebangsaan Malaysia, 43600 Bangi, Selangor Darul Ehsan, Malaysia
[b] Grenoble Institute of Technology, The International School of Paper, Print Media and Biomaterials (PAGORA), BP65, 38402 Saint Martin d'Hères Cedex, France

ARTICLE INFO

Article history:
Received 5 May 2012
Received in revised form
26 November 2012
Accepted 27 November 2012
Available online 17 December 2012

Keywords:
Kenaf
Cellulose nanocrystals
Cassava starch
Mechanical properties

ABSTRACT

Biodegradable materials made from cassava starch and kenaf fibers were prepared using a solution casting method. Kenaf fibers were treated with NaOH, bleached with sodium chlorite and acetic buffer solution, and subsequently acid hydrolyzed to obtain cellulose nanocrystals (CNCs). Biocomposites in the form of films were prepared by mixing starch and glycerol/sorbitol with various filler compositions (0–10 wt%). X-ray diffraction revealed that fiber crystallinity increased after each stage of treatment. Morphological observations and size reductions of the extracted cellulose and CNCs were studied using field emission scanning electron microscopy and transmission electron microscopy. The effects of different treatments and filler contents of the biocomposites were evaluated through mechanical tests. Results showed that the tensile strengths and moduli of the biocomposites increased after each treatment and the optimum filler content was 6%.

1. Introduction

Natural source based composites are considered to be promising substitutes or complements to their non-biodegradable petrochemical-based counterparts (Siracusa, Rocculi, Romani, & Rosa, 2008). The best known materials for making these green materials are starch and cellulose (John & Thomas, 2008). Both of these materials are renewable and can be obtained abundantly from different sources. Furthermore, the lower costs and the biodegradability of these resources have generated great interest in terms of their use in packaging applications (Fama, Flores, Gerschenson, & Goyanes, 2006; Petersson, Kvien, & Oksman, 2007; Teixeira et al., 2009). Even so, a noble plastic made from plasticized starch film can only be realized if the poor resistance to humidity that causes the deterioration of its mechanical properties is overcome (Svagan, Hedenqvist, & Berglund, 2009). Previous studies demonstrated that tailoring starch with cellulose helps to minimize this problem and bring about an improvement in thermal stability (Chen, Liu, Chang, Cao, & Anderson, 2009; Teixeira et al., 2009).

Starch is a natural polymer consisting of amylose and amylopectin. Among the major sources of starch are maize, cassava, sweet potato, yam, corn, rice, oats, and peas (Chen et al., 2009; Galdeano, Mali, Grossmann, Yamashita, & Garcia, 2009; Van Beilen & Poirier, 2007). In nature, starch can be solubilized in the presence of water and/or a plasticizer followed by heating and mixing, which produces a substance known as thermoplastic starch (TPS) (Cyras, Manfredi, Ton-That, & Vazquez, 2008; Schlemmer, Sales, & Resck, 2009). When a starch suspension is heated, semicrystalline TPS granules start to swell and absorb water, which is accompanied by the destruction of hydrogen bonds between the macromolecules (Che, Wang, Ozkan, Chen, & Mao, 2008; Yang, Yu, & Ma, 2006). In recent years, starch has found use in the food industry, and its modified forms have been employed in industrial packaging materials, disposable cups, and also in pharmaceuticals (Casas, Ferrero, de Paz, & Jiminez-Castellanos, 2009; Schlemmer & Sales, 2010).

Cellulose, which is one of the main components in most natural fibers, is composed of repeating D-glucopyranose units. It is a semicrystalline natural polymer that exhibits both amorphous and crystalline phases. Siro and Plackett (2010) reported that the diameter of celluloses fibril is between 5 and 10 nm while the length is dependent on the source of the cellulose. Nowadays, it is common practice among researchers to use this linear semicrystalline polysaccharide as a nano-reinforcer in composites. This is not just because of the good mechanicals properties imparted by the nano-sized cellulose but also due to its high aspect ratio (L/D) and its ability to form continuous networks (Habibi, El-Zawawy, Ibrahim, & Dufresne, 2008; Li, Tabil, & Panigrahi, 2007; Svagan et al., 2009). Lee et al. (2009) concluded that nano-sized cellulose has many advantages owning to its high stiffness and high specific area.

* Corresponding author. Tel.: +60 3 89215431; fax: +60 3 89215410.
E-mail address: gading@ukm.my (I. Ahmad).

0144-8617/$ – see front matter © 2012 Elsevier Ltd. All rights reserved.
http://dx.doi.org/10.1016/j.carbpol.2012.11.106

Table 1
Codification of materials.

Designation	Materials
K	Kenaf
KA	Alkali treated kenaf
KB	Bleached kenaf
CNCs	Cellulose nanocrystals
CS	Cassava starch
TPCS	Thermoplastic cassava starch
TPCS-K	Thermoplastic cassava starch/raw kenaf
TPCS-KA	Thermoplastic cassava starch/alkali treated kenaf
TPCS-KB	Thermoplastic cassava starch/bleached kenaf
TPCS-CNCs	Thermoplastic cassava starch/cellulose nanocrystals

Kenaf or *Hibiscus cannabinus* is a natural tropical plant that is grown commercially in many places around the world and is among the crops that are a potential source of revenue for developing countries including Malaysia. Physically, kenaf stem has a cylindrical structure consisting of two types of fibers, the core (internal fiber) and the bark (outer fiber). The pith of kenaf fibers can be equated with the fibers found in hard wood (Mohd Edeerozey, Md Akil, Azhar, & Zainal Ariffin, 2007). It was reported that the lignin content in kenaf ranges between 5.9 and 19% while that of hemicellulose is between 15 and 23%. Cellulose constitutes the major content and ranges between 44 and 63.5% (Jonoobi, Harun, Shakeri, Misra, & Oksman, 2009; Sanadi, Hunt, Caufield, Kovascvolgi, & Destree, 2001; Zampaloni et al., 2007).

The objective of this investigation was to show the potential of using multiscale kenaf fibers after alkalization, bleaching, and hydrolysis treatments as a reinforcing agent in thermoplastic cassava starch-kenaf biocomposites. In order to present comparable results, the variation of filler loading for each treatment was used to study the properties of the composites.

2. Experimental

2.1. Materials

Kenaf fiber was provided by Kenaf Fiber Industry Sdn. Bhd. (Malaysia) and native cassava starch (CS) was supplied by Thye Huat Chan Sdn. Bhd. (Malaysia). Sulfuric acid (98%), sodium hydroxide (99%), sodium chlorite (80%), and glacial acetic acid (99.5%) were purchased from SYSTERM-chemAR (Malaysia) and Sigma–Aldrich (Germany). All of the chemicals were used without purification. Laboratory grade sorbitol (98%, Sigma–Aldrich) and glycerol (99.5%, SYSTERM-chemAR) were used as plasticizers for preparing the biocomposites. Membranes 1 inch × 10 feet (Carolina Dialysis Tubing, NC) for dialysis were used as received. The abbreviations that are used to designate the materials are shown in Table 1.

2.2. Preparation of cellulose nanocrystals from kenaf fibers

Cellulose nanocrystals (CNCs) from kenaf were prepared by acid hydrolysis of the cellulose obtained as described elsewhere (Kargarzadeh et al., 2012). Briefly, kenaf fibers were vigorously stirred in a 4% alkali solution at 80 °C for 3 h. This process was repeated three times. Afterward, bleaching was performed three times with 1.7% sodium chlorite solution and acetic acid buffer solution for 4 h at 80 °C. Hydrolysis was conducted at 45 °C with 65% sulfuric acid. The time for hydrolysis in this research was fixed at 40 min, which was found previously to be optimum (Kargarzadeh et al., 2012). The process was terminated by placing the reaction flask into an ice bath. The excess sulfuric acid was then removed by repeated centrifugation at 10,000 rpm for 10 min. Following this, the resulting suspension was dialyzed against distilled water using a cellulose membrane for 2 weeks. The final suspension had a pH of 6.

2.3. Preparation of composite films

Fabrication of thermoplastic cassava starch-raw kenaf (TPCS-K), thermoplastic cassava starch-alkali treated kenaf (TPCS-KA), thermoplastic cassava starch-bleached kenaf (TPCS-KB), and thermoplastic cassava starch-cellulose nanocrystals (TPCS-CNCs) biocomposite films was based on solution casting according to previous study with modifications (Fama et al., 2006). CS was first mixed with sorbitol and glycerol (50:50) in distilled water and heated at ~71 °C under continuous stirring until the mixture had gelatinized. After this, composites with different fiber loading (2%, 4%, 6%, 8%, and 10 wt%; dry starch basis) were prepared by the addition of aqueous suspension. The final water content was adjusted to 20 wt% (water + suspension on a dry starch basis) for all of the samples. Each mixture was cast into a Petri dish and left overnight in an oven before being kept at room temperature in a conditioning desiccator at 30% relative humidity prior to testing. The thicknesses of the processed samples were fixed to produce 250–300-μm-thick plates.

2.4. Microscopic analysis

The morphology of the fibers after each treatment was investigated using a Zeiss Supra 55VP field emission scanning electron microscopy (FESEM) at a magnification of 400×. The filler/matrix interface was also studied using the same microscope. The composite films were frozen in liquid nitrogen and broken into small pieces. All the samples were mounted on aluminum stub by double-faced tape, coated with gold before observation to prevent charging with thickness around 0.01–0.1 μm (Sputter Coater model BioRAD, 2.2 kV, 2 min) and observed using an applied tension of 10 kV.

Transmission electron microscopy (TEM) was conducted using a Philips CM30 microscope to investigate the morphology of the hydrolyzed kenaf. A droplet of diluted suspension was deposited onto a Cu grid covered with a thin carbon film. To enhance the contrast, the nanocrystals were negatively stained with 2 wt% uranyl acetate (a heavy metal salt) solution in deionized water for 1 min and then dried at room temperature. In total, 100 fibers from each treatment were measured and the results were reported as the mean value of the data for each measurement.

2.5. X-ray diffraction

The wide-angle-X-ray diffraction (XRD) patterns of K, KA, KB, and freeze dried CNCs were recorded on a Bruker AXS X-ray diffraction instrument using monochromatic CuKα radiation (λ = 0.154 nm) generated at 40 kV and 40 mA. Scattered radiation was detected in the range for Bragg's angle 2θ of 10–70°. The crystallinity index (CrI) of each sample was determined using Eq. (1)

$$\mathrm{CrI}\ \ (\%) = \frac{I_{002} - I_{\mathrm{am}}}{I_{002}} \times 100 \qquad (1)$$

where I_{002} is the maximum intensity of the (0 0 2) lattice diffraction peak and I_{am} is the intensity scattered by the amorphous part of the sample.

2.6. Thermogravimetric analysis

Thermogravimetric analysis (TGA) and differential thermogravimetry (DTG) were carried out with a Mettler Toledo thermogravimetric analyzer (TGA/SDTA 85-F) in a nitrogen atmosphere for each matrix and the optimum composite films from each

set of treatments. The samples were heated from 25 °C to 600 °C at 10 °C min^{-1}.

2.7. Mechanical testing

The mechanical performance of the films was evaluated in terms of tensile strength and tensile modulus using a universal testing machine (Instron model 5566, USA) at room temperature according to ASTM D882. A crosshead speed of 50 mm/min, initial grip distance of 40 mm, and load cell of 50 N were used for this test. The film thickness was determined at five points using a digital caliper (Mitutoyo, ±1 μm). The average thickness of the samples was 0.27 ± 0.02 mm. The samples were cut into a dumbbell shape and the average value of seven replicates for each sample was taken. The tensile test characteristics were calculated using Bluehill software.

3. Results and discussion

3.1. Fiber morphology

Fig. 1 presents field emission scanning electron microscope FESEM images of kenaf fiber after different stages of treatment. A rough surface with impurities was clearly observed for the K fiber. However, after alkalization the rough surface of the raw fibers was destroyed. It was replaced by a smooth surface with relatively less impurities due to the removal of most of the hemicellulose, some lignin, and waxy materials that covered the peripheral surface of the fiber cell wall (Li et al., 2007; Sgriccia, Hawley, & Misra, 2008). In addition, the kenaf fiber bundle also started to separate into thinner fibers. As discussed earlier, the alkalization not only eliminated the highly branched hemicellulose and some of the lignin but also decreased the fiber dimension leading to produce finer fibrillar structures. During hot alkaline treatment, hemicellulose is hydrolyzed and part of the lignin undergoes depolymerization. The morphology for KA was the same as that obtained by Kim and Netravali (2010) through sisal alkalization.

For KB, more significant changes of the fiber surface were observed. Further fibrilation of the fibers was seen due to the loss of lignin that was left in the fibers. The use of the bleaching agent $NaClO_2$ and acetic buffer solution eliminated the lignin by oxidizing it, which led to its dissolution in alkaline medium and then fiber fibrilation (Bhatnagar & Sain, 2005; Keshk, Suwinarti, & Sameshima, 2006).

3.2. Cellulose nanocrystal morphology

Fig. 2 shows TEM images for the CNCs obtained after acid hydrolysis under different magnifications. The hydrolyzed cellulose resulted in needle-like shapes in agreement with previous studies (Liu, Zhong, Chang, Li, & Wu, 2010; Oksman, Mathew, Bondeson, & Kvien, 2006). This treatment dissolved the low lateral order amorphous domain, leaving the highly crystalline region intact. From these images, we could see that most of the fibrils were separated but that some were still agglomerated. In addition, there were also clear spots that arose from uranyl staining. The diameter of individual CNCs was 12 ± 3.4 nm and the length was between 70 and 190 nm with an aspect ratio (L/D) of 13.2 (Kargarzadeh et al., 2012).

3.3. Crystallinity

Fig. 3 shows the XRD patterns of original kenaf, KA, KB, and CNCs obtained after sulfuric acid hydrolysis. The crystallinity index, (CrI) were calculated as described in Section 2 and the results are shown in Table 2. A gradual increase in crystallinity for the treated fibers and CNCs was observed with CNCs having the highest CrI followed by KB, KA, and K. The increasing trend was due to pre-acid treatments that successfully eliminated the non-cellulosic materials in the kenaf fibers, which existed in the amorphous regions, leading to realignment of the cellulose molecules (Li, Fei, Cai, Feng, & Yao, 2009). Moreover, an increase in the ratio of crystalline regions increased the rigidity of the cellulose fiber. According to Alemdar & Sain (2008), the higher crystallinity of the chemically treated cellulose fibers is associated with the higher tensile strength of the fibers. The higher diffraction peak of the treated kenaf as compared

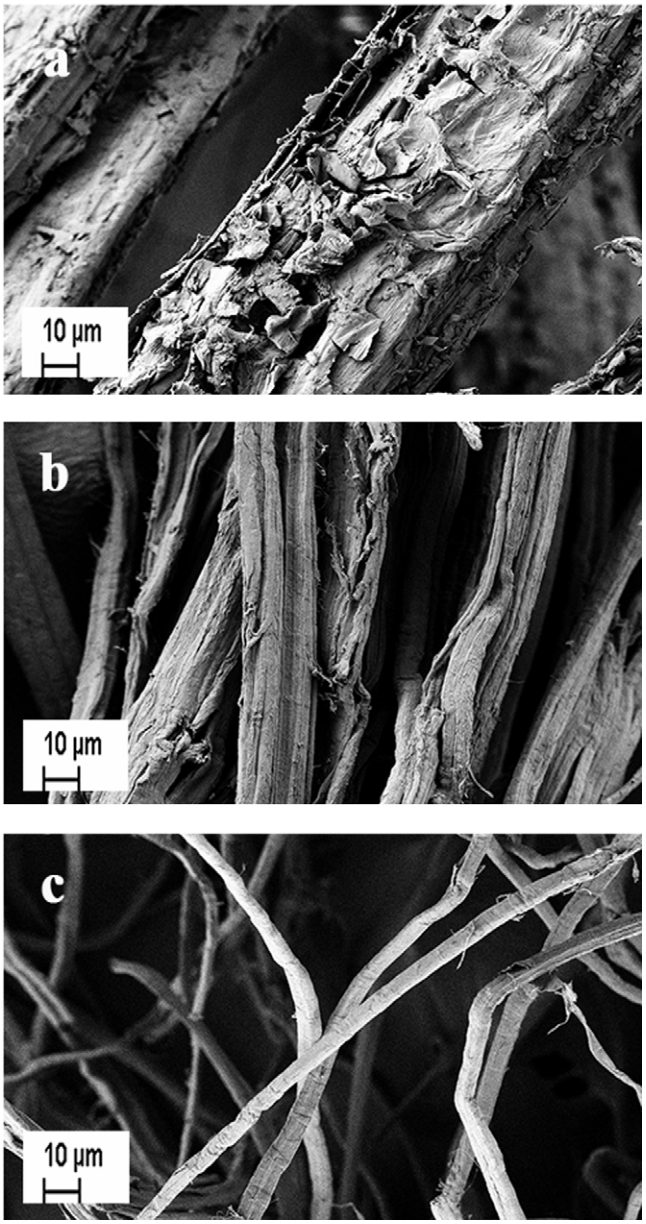

Fig. 1. FESEM micrographs of raw kenaf (a), alkali treated kenaf (b), and bleached kenaf (c).

Table 2
Crystallinity index (CrI) of each sample.

Type	CrI (%)
K	60.8
KA	68.2
KB	72.8
CNCs	81.8

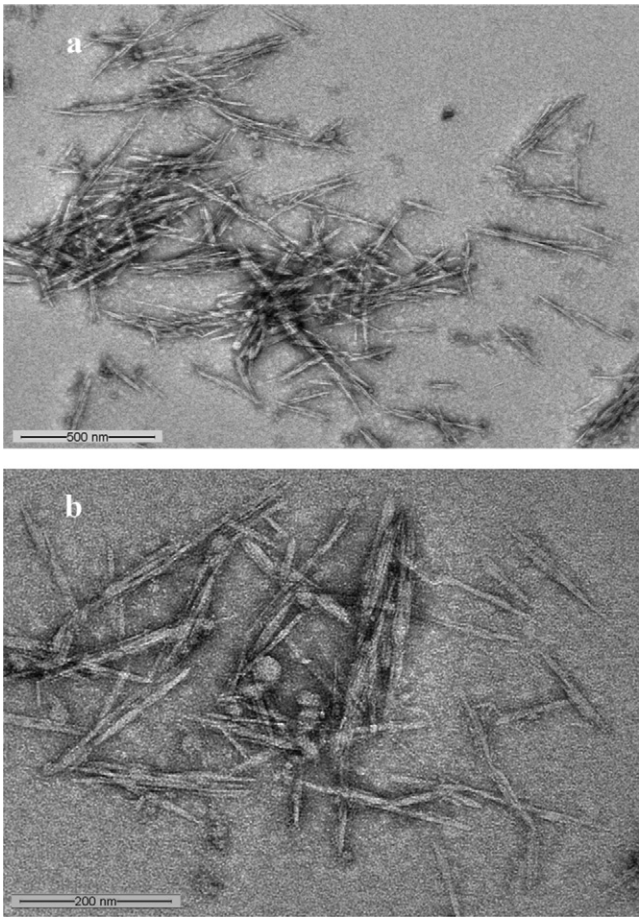

Fig. 2. TEM micrographs of hydrolyzed kenaf under different magnifications: 13,000× (a) and 35,000× (b).

to that for the raw kenaf also indicates the higher crystallinity in the structure of the treated fibers (Alemdar & Sain, 2008).

X-ray diffractometry profiles also illustrated that all of the fibers had the same crystalline form of cellulose I with three well-defined peaks at $2\theta = 16^\circ$, 22.5°, and 34.5°. KA showed a more intense peak compared to K. The sharp peaks were mainly because of the decrease in the interfibrillar regions due to the removal of hemicellulose and some of the lignin during alkalization. Sharper and higher peaks were observed for KB. This suggests that the elimination of most lignin in the fiber after bleaching caused the crystallinity to increase.

The intensities of the peaks for CNCs were still higher, showing that the CNCs samples were more crystalline than K, KA, and KB. The high crystallinity index and peak intensity displayed by CNCs was attributed to degradation of the amorphous domains in the cellulose through acid hydrolysis. During hydrolysis, hydronium ions penetrate into the amorphous regions of the cellulose, promoting the hydrolytic cleavage of glycosidic bonds and subsequently releasing individual crystallites (de Souza Lima & Borsali, 2004). This result is consistent with previous research where nanocellulose from cassava bagasse and cotton showed increasing diffraction peaks compared to their untreated forms (Pasquini, Teixeira, Curvelo, Belgacem, & Dufresne, 2010; Teixeira, Corrêa, de Oliveira, & Mattoso, 2010).

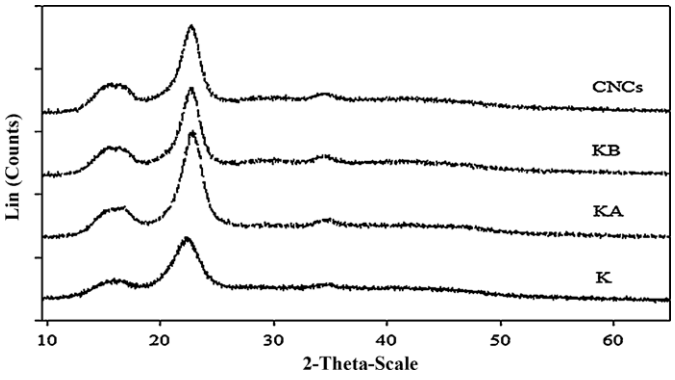

Fig. 3. X-ray diffractograms of untreated and treated kenaf fibers.

3.4. Morphological characterization of neat matrix and TPCS composites

The FESEM micrographs of TPCS, TPCS-K, TPCS-KA, TPCS-KB and TPCS-CNCs films with filler loading of 6 wt% are shown in Fig. 4. The effects of the surface treatments could be identified by the differences in the morphology of the fracture surfaces of the composite films. TPCS and TPCS-CNCs displays a relatively smoother surface compared to the composites reinforced with K, KA and KB. Rough surface displayed by these films are most likely due to the incorporation of the micro-scale fillers. As for TPCS, good interaction between the plasticizers and starch contribute to the continuous surface of the matrix. The smooth surface observed for TPCS-CNCs compared to other composite films indicates that CNCs, with a much smaller size, cannot be observed at this observation scale and are probably homogenously dispersed within TPCS since no aggregates can be seen. This fine dispersion of CNCs within the polymer matrix would results in an improvement in the mechanical properties of the nanocomposite compared to the TPCS and other composites. For TPCS-K (Fig. 4b), it is clear that the interfacial adhesion between the filler and matrix was poor. This can be readily seen from the absence of any physical contact between both components. The fibers are pulled out from the matrix and practically intact. Fracturing the sample did not lead to breaking the fiber. In addition, holes and spacing occur along the fiber, resulting in poor contact and inferior interfacial stress transfer. On the contrary, for TPCS-KA and TPCS-KB, the removal of hydrophobic hemicellulose and lignin provided a good wetting of the fiber, which can be observed from the near absence of holes around the fibers and breaking of the filler during fracture. The major component surrounding the fibers seems to be the continuous phase. Moreover, reduction of size and defibrillation of fiber bundles after alkalization and bleaching treatment allowed starchy materials to infiltrate inside it. Especially, TPCS-KB showed good interaction between the matrix and the fiber embedded and covered by the matrix and no void is observed. Matrix covering fibers and significant reduction of voids observed should result in improved mechanical properties for TPCS-KA and TPCS-KB compared to TPCS-K.

3.5. Mechanical properties

3.5.1. Tensile strength

The tensile strength of the films was determined and the results are plotted in Fig. 5(a). As shown, the film reinforced with treated fibers had a higher tensile strength compared to the neat matrix film, which had the lowest tensile strength (3.5 MPa). Compared to the neat matrix, no improvement was observed for TPCS-K.

The 6% TPCS-CNCs showed the highest tensile strength at 8.2 MPa among the composites for all of the fiber compositions. Acid hydrolysis resulted in an enhancement of 91–134% in terms of tensile strength compared to the control film. Even though there was a slight decrease (or stabilization) at 8% CNCs loading, which was most probably due to the aggregation of nanocrystals in the matrix phase, its tensile strength was still higher compared to the others

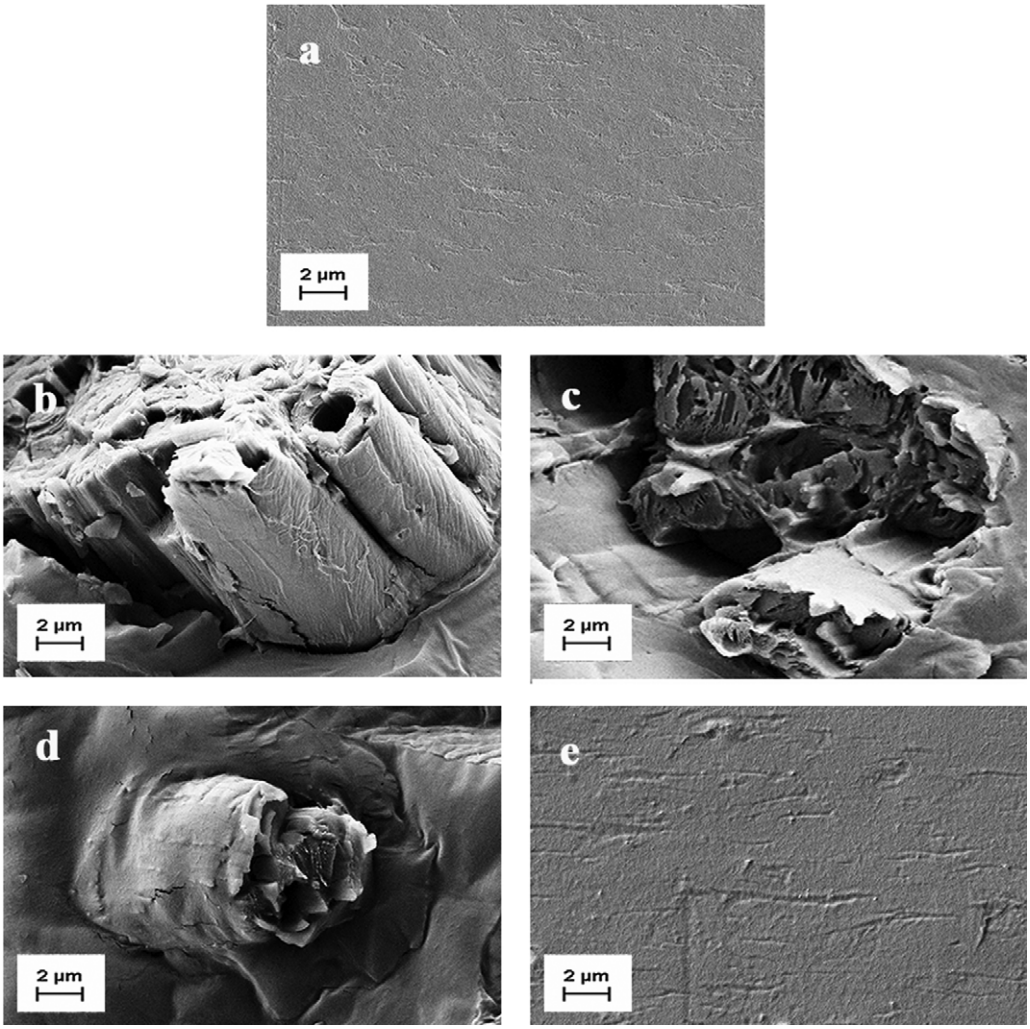

Fig. 4. FESEM micrographs of TPCS (a), TPCS-K (b), TPCS-KA (c), TPCS-KB (d), and TPCS-CNCs (e).

fillers. This significant improvement for TPCS-CNCs was mainly due to the high specific area and high L/D ratio, which provided better reinforcement capability. This also reflected the strong interfacial interaction that occurred between starch and cellulose. The ability of the nanofibers to restrict the matrix mobility also contributed to this improvement.

For TPCS-KA, and TPCS-KB, no significant evolution upon filler loading was observed but the tensile strength value was

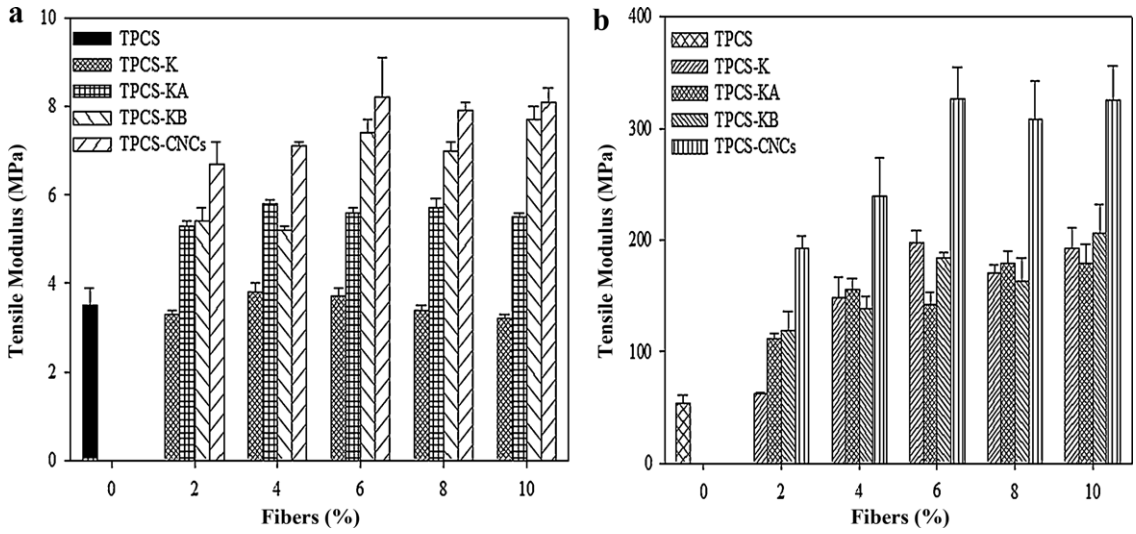

Fig. 5. Effects of fiber treatments on tensile strength (a) and tensile modulus (b).

systematically higher than for the neat matrix. This improvement was due to the strong interfacial interaction between starch and fibers, which brings about good stress transfer. On the other hand, the slight decrease for the composites at certain loadings was mainly due to entanglement of the fibers inside the matrix phase.

The TPCS-KB composites showed better mechanical characteristics compared to TPCS-KA. As seen in Fig. 1, the fibers were separated individually due to removal of most of the lignin, which led to good adhesion between the starch and the fibers. This effect was again merely due to the strong interfacial interaction and adhesion between the matrix and the fibers. This enhancement was also related to the higher crystallinity as described by Johar, Ahmad, and Dufresne (2012) who concluded that the increase in cellulose fiber crystallinity increases their stiffness and rigidity, and therefore strength.

3.5.2. Tensile modulus

Fig. 5(b) shows the tensile modulus values as a function of fiber loading. A clear tendency of increasing stiffness was observed for all of the composites with increasing fiber content. The addition of fibers contributed to reinforcement of the polymeric matrix and this was reflected in the stiffness of the composite (Dias, Muller, Larotonda, & Laurindo, 2011; Rezaur Rahman, Monimul Huque, Nazrul Islam, & Mahbub Hasan, 2008). Furthermore, the significant increase was attributed to the similarity between the chemical structures of cellulose and starch (Fahma, Imamoto, Hori, Iwata, & Takemura, 2011; Muller, Laurindo, & Yamashita, 2009). However, no clear trend can be observed upon fiber treatment when comparing TPCS-K, TPCS-KA and TPCS-KB contrarily to tensile strength. This is most probably due to the fact that the modulus is determined from the linear behavior of the composite, i.e. under low strain, and the interfacial adhesion is much less sollicitated.

For the TPCS-CNCs composites, an increasing trend in the elastic modulus of the films was observed with the addition of nanocellulose. It should be noted that TPCS-CNCs showed the highest stiffness for all filler compositions with 326.1 MPa. Starting from 6 wt% CNCs loading, the modulus tended to stabilize. Aggregates of CNCs in the matrix contributed to this phenomenon and hence restricted filler reinforcement.

For TPCS-CNCs, the increase in the tensile modulus may have been related to the increased stiffness due to the addition of CNCs (Lee et al., 2009). The high crystallinity of the CNCs as discussed from XRD experiments led to more rigid materials in the case of TPCS-CNCs and hence its high modulus. The high surface area displayed by this highly crystalline nanocellulose therefore increased the surface interaction between the filler and the matrix and led to mechanical improvement in term of its modulus.

3.6. Thermogravimetric analysis

Thermogravimetric analysis (TGA) was carried out to investigate the thermal stability of starch, TPCS matrix, and the TPCS composites. Fig. 6(a) presents the TGA experimental results. The optimum sample from each set of treatments was studied and compared to the pure matrix (4% for both TPCS-K and TPCS-KA, 10% and 6% for TPCS-KB and TPCS-CNCs, respectively). The evolution of the mass loss was similar for the CS, TPCS, and composites with two major breakdowns being observed. Weight loss starting from 50 °C to 150 °C was detected for the TPCS and TPCS composites. The TGA thermograms also showed that the temperatures of this thermal event for the matrix and composites were close to each other. This thermal event corresponded to evaporation of the water in the materials. Water absorption by the matrix and composites was rather high because water can penetrate into the H-bonding with OH groups of the glucosyl units along the polymer chain (Schlemmer & Sales, 2010). The decline in the weight loss

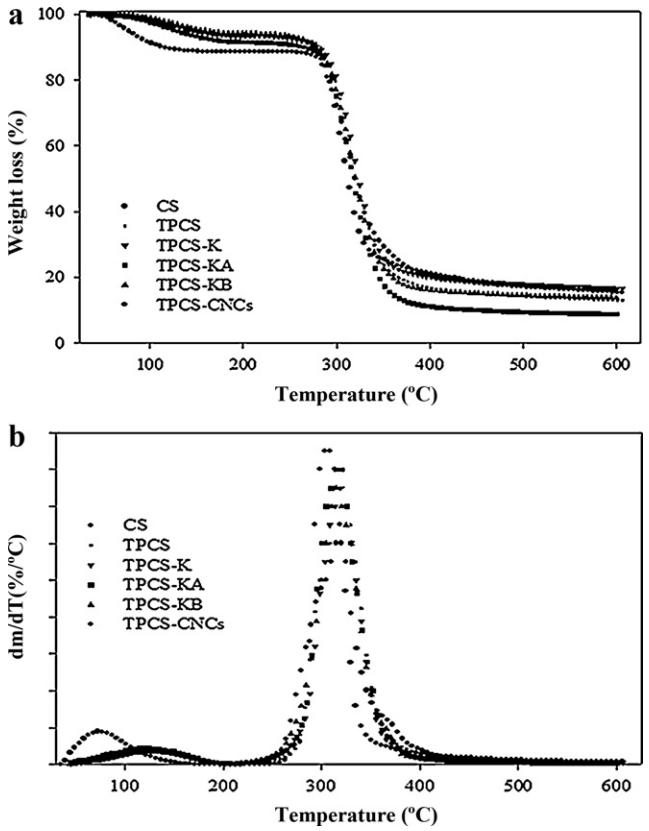

Fig. 6. TGA curves for CS, TPCS, and TPCS/composites (a), and DTG curves for CS, TPCS, and TPCS/composites (b).

of the TPCS and the composites was related to evaporation of the plasticizers.

For CS, its first degradation (room temperature until 110 °C) was due to the removal of water and moisture in starch (Kaewtatip & Tanrattanakul, 2008). Starch absorption of water and moisture are related to the hydrogen bonding formed by the glucose hydroxyl along the starch polymer chains (Schlemmer & Sales, 2010). Further degradation of CS occurred around 273–335 °C which ascribed the degradation of starch, due to random scission of the main chains (1,4-β-D-glucospyranose). Similar observation was also reported by Kaith, Jindal, Jana, and Maiti (2010) using corn starch as a matrix. Above 335 °C, the pyrolysis of starch occurred and the yield product included carbon monoxide, volatile organic compounds, and carbonaceous residues (Carvalho, Curvelo, & Agneli, 2001).

For the matrix and composites, the second thermal degradation stage occurred from 280 °C to 385 °C. As seen in Fig. 6(a), starch biocomposites after treatments have higher thermal degradation than CS. From the thermogram, it was also found that TPCS-K composite degrade earlier at higher temperature compared to others which could be explained by the low stability of hemicelluloses and lignin which present in the fibers. The higher thermal stability of TPCS-KA and TPCS-KB can be observed which is due to the removal of hemicellulose and lignin in the fibers after treatment thus improving its composite thermal stability compared to TPCS-K. As for TPCS-CNCs composite, the shifting to higher temperature is due to good interaction between CNCs and the matrix phase therefore helps to increase its thermal stability (Chang, Jian, Zheng, Yu, & Ma, 2010).

4. Conclusions

Kenaf fibers were treated with alkali and bleaching agent, and then acid hydrolysis was performed to obtain CNCs. The diameter

and length of the CNCs observed by TEM were 12 ± 3.04 nm and 70–190 nm, respectively. Cassava starch/kenaf biocomposite films were prepared via solution casting with glycerol/sorbitol as plasticizers. The reinforcing effect of the filler was investigated by associating different treatments and loading (2%, 4%, 6%, 8%, and 10 wt%) with the matrix. It was found that by increasing the loading composition, the mechanical properties were enhanced, with the biocomposite having 6% TPCS-CNCs showing the highest tensile strength at 8.2 MPa. This suggests the existence of good stress transfer and interfacial interactions between the matrix phase and the filler, which was related to the high L/D and efficiency of the fiber treatments, especially for TPCS-CNCs. These results also indicate that kenaf fibers are compatible with the matrix and can act as good reinforcing particles in the starch phase. An increasing trend of crystallinity for the fibers after the treatments was also observed through XRD analysis.

Acknowledgements

The authors would like to thank the Universiti Kebangsaan Malaysia (UKM) for providing a grant to make this research possible. We also thank the Ministry of Science and Technology, Malaysia (MOSTI), from which we received a National Science Fellowship (NSF) scholarship. The French Embassy in Kuala Lumpur is also acknowledged for financial support (French Scholars in Malaysia).

References

Alemdar, A., & Sain, M. (2008). Biocomposites from wheat straw nanofibers: Morphology, thermal and mechanical properties. *Composites Science and Technology*, *68*, 557–565.

Bhatnagar, A., & Sain, M. (2005). Processing of cellulose nanofiber-reinforced composites. *Journal of Reinforced Plastics and Composites*, *24*, 1259–1268.

Carvalho, A. J. F., Curvelo, A. A. S., & Agneli, J. A. M. (2001). A first insight on composites of thermoplastics starch and kaolin. *Carbohydrate Polymers*, *45*, 189–194.

Casas, M., Ferrero, C., de Paz, M. V., & Jiminez-Castellanos, M. R. (2009). Synthesis and characterization of new copolymers of ethyl methacrylate grafted on tapioca starch as novel excipients for direct compression matrix tablets. *European Polymer Journal*, *45*(6), 1765–1776.

Chang, P. R., Jian, R., Zheng, P., Yu, J., & Ma, X. (2010). Preparation and properties of glycerol plasticized-starch (GPS)/cellulose nanoparticle (CN) composites. *Carbohydrate Polymers*, *79*, 301–305.

Che, L., Wang, L., Ozkan, N., Chen, X. D., & Mao, Z. (2008). Rheological properties of dilute aqueous solutions of cassava starch. *Carbohydrate Polymers*, *74*, 385–389.

Chen, Y., Liu, C., Chang, P. C., Cao, X., & Anderson, D. P. (2009). Bionanocomposites based on pea starch and cellulose nanowhiskers hydrolyzed from pea hull fibre, effect of hydrolysis time. *Carbohydrate Polymers*, *76*, 607–615.

Cyras, V. P., Manfredi, L. B., Ton-That, M., & Vazquez, A. (2008). Physical and mechanical properties of thermoplastic starch/montmorillonite nanocomposite films. *Carbohydrate Polymers*, *73*, 55–63.

de Souza Lima, M. M., & Borsali, R. (2004). Rodlike cellulose microcrystals, structure, properties, and applications. *Macromolecular Rapid Communications*, *25*, 771–787.

Dias, A. B., Muller, C. M. O., Larotonda, F. D. S., & Laurindo, J. B. (2011). Mechanical and barrier properties of composite films based on rice flour and cellulose fibers. *Food Science and Technology*, *44*, 535–542.

Fahma, F., Imamoto, S., Hori, N., Iwata, T., & Takemura, A. (2011). Effect of pre-acid hydrolysis treatment on morphology and properties of cellulose nanowhiskers from coconut husk. *Cellulose*, *18*, 443–450.

Fama, L., Flores, S. K., Gerschenson, L., & Goyanes, S. (2006). Physical characterization of cassava starch biofilms with special reference to dynamic mechanical properties at low temperature. *Carbohydrate Polymers*, *66*, 8–15.

Galdeano, M. C., Mali, S., Grossmann, M. V. E., Yamashita, F., & Garcia, M. A. (2009). Effects of plasticizers on the properties of oat starch films. *Materials Science and Engineering C*, *29*, 532–538.

Habibi, Y., El-Zawawy, W. K., Ibrahim, M. H., & Dufresne, A. (2008). Processing and characterization of reinforced polyethylene composites made with lignocellulosic fibers from Egyptian agro-industrial residues. *Composites Science and Technology*, *68*, 1877–1885.

Johar, N., Ahmad, I., & Dufresne, A. (2012). Extraction, preparation and characterization of cellulose fibres and nanocrystals from rice husk. *Industrial Crops and Products*, *37*, 93–99.

John, M. J., & Thomas, S. (2008). Biofibre and biocomposites. *Carbohydrate Polymers*, *71*, 343–364.

Jonoobi, M., Harun, J., Shakeri, A., Misra, M., & Oksman, K. (2009). Chemical composition, crystallinity, and thermal degradation of bleached and unbleached kenaf bast (*Hibiscus cannabinus*) pulp and nanofibers. *BioResources*, *4*(2), 626–639.

Kaith, B. S., Jindal, R., Jana, A. K., & Maiti, M. (2010). Development of corn starch based green composites reinforced with *Saccharum spontaneum* L fiber and graft copolymer – Evaluation of thermal, physico-chemical and mechanical properties. *Bioresource Technology*, *101*, 6843–6851.

Kaewtatip, K., & Tanrattanakul, V. (2008). Preparation of cassava starch grafted with polystyrene by suspension polymerization. *Carbohydrate Polymers*, *73*, 647–655.

Kargarzadeh, H., Ahmad, I., Abdullah, I., Dufresne, A., Zainudin, S. Y., & Sheltami, R. M. (2012). Effect of hydrolysis conditions on the morphology, crystallinity, and thermal stability of cellulose nanocrystals extracted from kenaf bast fibers. *Cellulose*, *19*, 855–866.

Keshk, S., Suwinarti, W., & Sameshima, K. (2006). Physicochemical characterization of different treatment sequences on kenaf bast fiber. *Carbohydrate Polymer*, *65*, 202–206.

Kim, J. T., & Netravali, A. N. (2010). Mercerization of sisal fibers, Effect of tension on mechanical properties of sisal fiber and fiber-reinforced composites. *Composites, Part A*, *41*, 1245–1252.

Lee, S. Y., Jagan, M. D., Kang, I., Doh, G., Lee, S., & Han, S. O. (2009). Nanocellulose reinforced PVE composite films, effects of acid treatment and filler loading. *Fibers and Polymers*, *10*, 77–82.

Li, X., Tabil, L. G., & Panigrahi, S. (2007). Chemical treatments of natural fiber for use in natural fiber-reinforced composites: A review. *Journal Polymer Environment*, *15*, 25–33.

Li, R., Fei, J., Cai, Y., Feng, J., & Yao, J. (2009). Cellulose whiskers extracted from mulberry. A novel biomass production. *Carbohydate Polymer*, *76*, 94–99.

Liu, D., Zhong, T., Chang, P. R., Li, K., & Wu, Q. (2010). Starch composite reinforced by bamboo cellulosic crystals. *Bioresource Technology*, *101*, 2529–2536.

Mohd Edeerozey, A. M., Md Akil, H., Azhar, A. B., & Zainal Ariffin, M. I. (2007). Chemical modifications of kenaf fibers. *Materials Letters*, *61*, 2023–2025.

Muller, C. M. O., Laurindo, J. B., & Yamashita, F. (2009). Effect of cellulose fibers addition on the mechanical properties and water vapor barrier of starch-based films. *Food Hydrocolloids*, *23*, 1328–1333.

Oksman, K., Mathew, A. P., Bondeson, D., & Kvien, I. (2006). Manufacturing process of cellulose whiskers/polylactic acid nanocomposites. *Composites Sciences and Technology*, *66*, 2776–2784.

Pasquini, D., Teixeira, E. D. M., Curvelo, A. A. D. S., Belgacem, M. N., & Dufresne, A. (2010). Extraction of cellulose whiskers from cassava bagasse and their application as reinforcing agent in natural rubber. *Industrial Crops and Products*, *32*, 486–490.

Petersson, L., Kvien, I., & Oksman, K. (2007). Structure and thermal properties of poly(lactic acid)/cellulose whiskers nanocomposite materials. *Composite Science and Technology*, *67*, 2535–2544.

Rezaur Rahman, Md., Monimul Huque, Md., Nazrul Islam, Md., & Mahbub Hasan. (2008). Improvement of physico-mechanical properties of jute fiber reinforced polypropylene composites by post-treatment. *Composites, Part A*, *39*, 1739–1747.

Sanadi, A. R., Hunt, F., Caufield, D. F., Kovascvolgi, G., & Destree, B. (2001). High fiber low matrix composites: Kenaf fiber/polypropylene. In *The sixth international conference on woodfiber-plastic composite, Wisconsin*.

Schlemmer, D., Sales, M. J. A., & Resck, I. S. (2009). Degradation of different polystyrene/thermoplastic starch blends buried in soils. *Carbohydrate Polymers*, *75*, 8–62.

Schlemmer, D., & Sales, M. J. A. (2010). Thermoplastic starch films with vegetable oils of Brazilian Cerrado. Thermal characterization. *Journal of Thermal Analysis and Calorimetry*, *99*, 675–679.

Sgriccia, N., Hawley, M. C., & Misra, M. (2008). Characterization of natural fiber surfaces and natural fiber composites. *Composites Part A: Applied Science and Manufacturing*, *39*, 1632–1637.

Siracusa, V., Rocculi, P., Romani, S., & Rosa, M. D. (2008). Biodegradable polymers for food packaging, a review. *Trends in Food Science & Technology*, *19*, 634–643.

Siro, I., & Plackett, D. (2010). Microfibrillated cellulose and new nanocomposite materials, a review. *Cellulose*, *17*, 459–494.

Svagan, A. J., Hedenqvist, M. S., & Berglund, L. (2009). Reduce water vapour sorption in cellulose nanocomposites with starch matrix. *Composites Science and Technology*, *69*, 500–506.

Teixeira, E. M., Corrêa, A. C., de Oliveira, C. R., & Mattoso, L. H. C. (2010). Cellulose nanofibers from white and naturally colored cotton fibers. *Cellulose*, *17*(3), 595–606.

Teixeira, E. M., Pasquini, D., Curvelo, A. A. S., Corradini, E., Belgacem, M. N., & Dufresne, A. (2009). Cassava bagasse cellulose nanofibrils reinforced thermoplastic cassava starch. *Carbohydrate Polymers*, *78*, 422–431.

Van Beilen, J. B., & Poirier, Y. (2007). Prospects for biopolymers production in plants. *Advances in Biochemical Engineering/Biotechnology*, *107*, 133–151.

Yang, J., Yu, J., & Ma, X. (2006). Study on the properties of ethylenebisformamide and sorbitol plasticized corn starch (ESPTPS). *Carbohydrate Polymers*, *66*, 110–116.

Zampaloni, M., Pourboghrat, F., Ayankovich, S., Rodgers, B. N., Moore, J., Drzal, L. T., Mohanty, A. K., & Misra, M. (2007). Kenaf natural rubber reinforced polypropylene composites: A discussion on manufacturing problems and solutions. *Composites Part A: Applied Science and Manufacturing*, *38*, 1569–1580.